Proc. Natl. Acad. Sci. USA
Vol. 90, pp. 7666–7670, August 1993
Developmental Biology

Local alterations of *Krox-20* and *Hox* gene expression in the hindbrain suggest lack of rhombomeres 4 and 5 in homozygote null *Hoxa-1* (*Hox-1.6*) mutant embryos

(homeobox gene/mouse development/mouse mutant/*in situ* hybridization)

PASCAL DOLLÉ*, THOMAS LUFKIN*, ROBB KRUMLAUF†, MANUEL MARK*, DENIS DUBOULE‡, AND PIERRE CHAMBON*§

*Laboratoire de Génétique Moléculaire des Eucaryotes du Centre National de la Recherche Scientifique, Unité 184 de Biologie Moléculaire et de Génie Génétique de l'Institut National de la Santé et de la Recherche Médicale, Institut de Chimie Biologique, Faculté de Médecine, 11 rue Humann, 67085 Strasbourg-Cedex, France; †National Institute of Medical Research, The Ridgeway, Mill Hill, London NW7 1AA, United Kingdom; and ‡European Molecular Biology Laboratory, Meyerhofstrasse 1, Postfach 10 2209, D6900 Heidelberg, Federal Republic of Germany

Contributed by Pierre Chambon, April 28, 1993

ABSTRACT **It is unknown whether cross-regulatory interactions between homeotic genes, which have been shown to play an important role in the maintenance of their expression domains during *Drosophila* development, are also important during mammalian development. We have analyzed here the expression of *Hox* genes in *Hoxa-1* (*Hox-1.6*) null mutant embryos to investigate the possible existence of regulatory interactions between *Hoxa-1* and other *Hox* genes. We show that the absence of a functional *Hoxa-1* gene product does not globally interfere with the expression of other *Hox* genes in terms of both spatial boundaries and transcript abundance. However, a limited area of the hindbrain shows a strong reduction in *Hoxb-1* (*Hox-2.9*) and *Krox-20* transcripts, which most likely reflects a marked reduction in size of the former fourth and fifth rhombomeres. These alterations coincide with the region that is subsequently affected in *Hoxa-1* null mutant mice and suggest that the primary defects in this mutation are spatially restricted deletions of some rhombomeric structures.**

The mammalian genome contains 38 genes (the *Hox* genes), which harbor a homeobox related to those of *Drosophila* homeotic genes of the Antennapedia and Bithorax complexes. *Hox* genes are clustered in four loci (the *HOX* complexes), whose structural organization is highly similar to that of *Drosophila* homeotic complexes (refs. 1–3; reviewed in refs. 4 and 5). The expression of murine *Hox* genes is coordinately regulated during embryogenesis, such that they are expressed along the embryo anteroposterior axis in overlapping domains, whose extent is related to the position of the gene within its complex (6). In addition, a subset of *Hox* genes display coordinate expression during limb and genital bud development (7–9). Experiments involving either the ectopic expression (10–12), or the disruption by gene targeting techniques (13–16), of various *Hox* genes support the idea that *Hox* genes could encode the positional information required for regional patterning along the various embryonic axes.

Cross-regulatory interactions are an important feature of the regulation of *Drosophila* homeotic genes (e.g., refs. 17–19). The existence of similar cross-regulatory interactions between mammalian *Hox* genes has been postulated and supported by the presence in some *Hox* promoters of binding sites for *Hox* gene products that are functional in cell culture systems (20, 21). We have investigated here whether such interactions may occur during mouse development. To this end, we have analyzed the pattern of expression of a number of *Hox* genes in homozygote null mutant embryos derived from a mouse strain that harbors a disrupted *Hoxa-1* (*Hox-1.6*) gene (14).

Two loss-of-function mutations have been established independently in *Hoxa-1* (14, 15), which is one of the earliest and most anteriorly expressed *Hox* genes (1, 22). Homozygous animals die at birth and earlier examination revealed that gestational day 18.5 *Hoxa-1*$^{-/-}$ fetuses have defects restricted to the hindbrain epithelium at the level of rhombomeres (r) 4–7, as well as to the corresponding neurogenic neural crest derivatives, the inner and middle ear, and the occipital bones of the skull (14). Although no gross externally visible alteration of the rhombomeric pattern was initially observed in day-9.5 *Hoxa-1*$^{-/-}$ embryos (14), the phenotypes suggested that there could be alterations to underlying segmentation. Systematic morphological examination of the hindbrain region of day-8 to -9 mutant embryos has revealed that only four rhombomere boundaries are present, thus defining five putative rhombomeres ("hindbrain segments"; ref. 23), whereas the normal embryo has seven rhombomeres (31). The otic vesicle or otocyst is present in *Hoxa-1*$^{-/-}$ embryos; however, it is reduced in size and more distant from the neuroepithelium than in normal embryos and is apparently shifted anteriorly, so that it now faces the fourth morphologically visible rhombomere (31). These early alterations of the hindbrain and otocyst appear to be the basis for the morphological abnormalities seen at later stages in the myelencephalon, some cranial nerves, and the ear (14, 15).

To examine early changes in hindbrain segmentation at the molecular level, as well as *Hox* gene regulation in this mutant background, we have investigated here the expression of several *Hox* genes and of the *Krox-20* gene in *Hoxa-1*$^{-/-}$ embryos. Segment-restricted alterations in gene expression have been found in this study, which correlate with the anatomic alterations caused by the mutation. However, these alterations do not appear to result from direct cross-regulatory effects of the *Hoxa-1* gene product on other *Hox* genes. These altered patterns of gene expression are helpful in further defining the early molecular events in hindbrain segments that are modified in *Hoxa-1*$^{-/-}$ embryos, as well as in understanding the role of *Hoxa-1* in development.

MATERIALS AND METHODS

Embryo Genotyping and RNA Probes. The targeted *Hoxa-1* mutation and the resulting phenotype have been described (14). Embryos from *Hoxa-1*$^{+/-}$ heterozygote crosses were

The publication costs of this article were defrayed in part by page charge payment. This article must therefore be hereby marked "*advertisement*" in accordance with 18 U.S.C. §1734 solely to indicate this fact.

Abbreviations: E8.5, embryonic day 8.5; r3, rhombomere 3.

§To whom reprint requests should be addressed.

dissected out at embryonic day (E) 8.5, 9.5, 10.5, and 12.5. Extraembryonic membranes were frozen for subsequent genotyping, and the embryos were fixed in 4% paraformaldehyde, dehydrated, and paraffin-embedded for subsequent *in situ* hybridization. Genotypes were determined by Southern blot analysis of extraembryonic membrane DNA, using specific *Hoxa-1* DNA probes as described (14). The following various RNA probes were used: *Hoxa-4* (*Hox-1.4*) (6), *Hoxa-3* (*Hox-1.5*) (24), *Hoxb-1* (*Hox-2.9*), *Hoxb-2* (*Hox-2.8*), *Hoxb-3* (*Hox-2.7*), *Krox-20* (25), *Hoxa-2* (*Hox-1.11*), *Hoxd-1* (*Hox-4.9*) (26).

***In Situ* Hybridization.** E8.5 embryos ($Hoxa\text{-}1^{-/-}$, $n = 4$; controls, $n = 7$) were sectioned sagittally, and E9.5 embryos ($Hoxa\text{-}1^{-/-}$, $n = 12$; $Hoxa\text{-}1^{-/+}$, $n = 12$; $Hoxa\text{-}1^{+/+}$, $n = 8$) were cut along a frontal plane. All sections (5 μm thick) were collected and dispatched to three (for E8.5) or maximally four (for E9.5) series of slides. Thus, four probes could be compared over 20 μm of tissues. *In situ* hybridization, washing, and emulsion autoradiography were performed as described (27). No significant difference was observed in the labeling patterns of $Hoxa\text{-}1^{+/-}$ and $Hoxa\text{-}1^{+/+}$ embryos.

RESULTS

We have analyzed the expression of the *Hoxb-1* and *Hoxd-1* genes (paralogous to *Hoxa-1*) as well as of neighboring genes belonging to either the *HoxA* (*Hoxa-2, -a-3, -a-4*) or *HoxB* (*Hoxb-2, -b-3*) complex (see Fig. 4*a*) in $Hoxa\text{-}1^{-/-}$ embryos, as well as $Hoxa\text{-}1^{-/+}$ heterozygote and $Hoxa\text{-}1^{+/+}$ wild-type littermates. An analysis of the transcripts of the *Krox-20* gene, which is specifically and transiently expressed in r3 and r5 (25), was also included. In all cases, the labeling patterns were identical in $Hoxa\text{-}1^{-/+}$ heterozygotes and wild-type animals, and both are subsequently referred to as control embryos. In late day-8.5 control embryos (E8.5), *Krox-20* transcripts were detected in both r3 and r5 (Fig. 1*a*), whereas $Hoxa\text{-}1^{-/-}$ littermate embryos showed a unique rhombomeric band of *Krox-20*-positive cells (Fig. 1*b*). From its location and from the perfect alignment between the *Krox-20* and the *Hoxb-2* anterior boundaries (Fig. 1*b*), this rhombomeric domain clearly corresponds to r3. However, posterior to the *Krox-20*-labeled r3, a thin stripe of cells located dorsally was labeled in both E8.5 and E9.5 mutant embryos, thus appearing as a vestige of r5 (see Figs. 2*b* and 3*b*; data not shown). In older E9.5 mutant embryos, *Krox-20* transcripts had almost disappeared from r3, as is the case in normal embryos (see Figs. 2*a* and 3*a*) and were consequently restricted to the vestigial r5 stripe (see Figs. 2*b* and 3*b*, arrows). A small population of mesenchymal *Krox-20*-labeled cells, which was connected to the r5 stripe and extended posteriorly, was detected in mutant embryos (Fig. 2*b*, arrowhead). The same type of *Krox-20*-labeled mesenchymal stripe was readily detected in control embryos, where it appeared connected to the posterior aspect of r5 (Fig. 3*a*, arrowheads). These cells probably correspond to the small population of r5-derived neural crest, which has been recently documented (28).

After an initial phase of widespread expression, the *Hoxb-1* gene is selectively expressed in r4 (29, 30). In E9.5 control embryos, *Hoxb-1* expression was specifically detected in r4, where its domain of expression was as wide as that of *Krox-20* in r5 (Fig. 2*a*). In contrast, in $Hoxa\text{-}1^{-/-}$ embryos, the *Hoxb-1* rhombomeric domain was severely reduced in size to a few dorsal cells located in between the *Krox-20*-expressing cells in r3 and the thin posterior stripe of *Krox-20*-positive cells (Fig. 2 *b* and *c*). These *Hoxb-1*-positive cells were thus restricted to a small dorsal area facing the constriction between the third and fourth rhombomeres (Fig. 2 *b* and *c*; see also Fig. 4*b*).

In E8.5 and E9.5 control embryos, *Hoxb-1* expression extended up to the r2/r3 boundary (Figs. 1*a* and 4*b*). The *Hoxb-2* anterior limit of expression appeared unaffected in mutant embryos, as it matched with that of *Krox-20* in r3 (Fig. 1*b*); the *Hoxb-2* transcript domain extended posteriorly in the same neural and mesenchymal tissues as in control embryos (compare Fig. 1 *a* and *b*). *Hoxa-2* is normally expressed up to r2, and maximally in r3 and r5, whereas *Hoxa-3* has a sharp cutoff aligned with the *Krox-20* boundary between r4/r5, and *Hoxa-4* shows a graded decrease in intensity up to r7 (refs. 25 and 26; Figs. 2*a*, 3*a*, and 4*b*). Interestingly, although $Hoxa\text{-}1^{-/-}$ embryos have an altered rhombomeric pattern, the expression domains of these *Hoxa* genes were not significantly affected (Figs. 2*b* and 3*b*). *Hoxa-2* transcripts extended up to r2, whereas the *Hoxa-3* transcript domain showed a boundary that was not as clearcut as in control embryos but nevertheless coincided with the position of the vestigial r5 as defined by the few labeled *Krox-20* cells (Figs. 2*b* and 3*b*). The *Hoxa-4* anterior boundary was correctly positioned—i.e., posterior to that of *Hoxa-3* (compare Fig. 3 *a* and *b*). In mutant embryos, the *Hoxb-3* expression boundary was aligned with that of *Hoxa-3* (data not shown), as described for normal embryos (25).

The expression of all the *Hox* genes studied here remained unaffected in all other parts of the body in E8.5 and E9.5 $Hoxa\text{-}1^{-/-}$ embryos. Specific *Hox* combinations in branchial arches (26) were preserved. For instance, *Hoxa-2* and *Hoxa-3* domains extended up to the second (b2) and third (b3) arches, respectively, as they did in control embryos (Fig. 3 *c* and *d*). In more-posterior regions, including the trunk, limb buds, and tail bud, *Hox* gene expression was indistinguishable

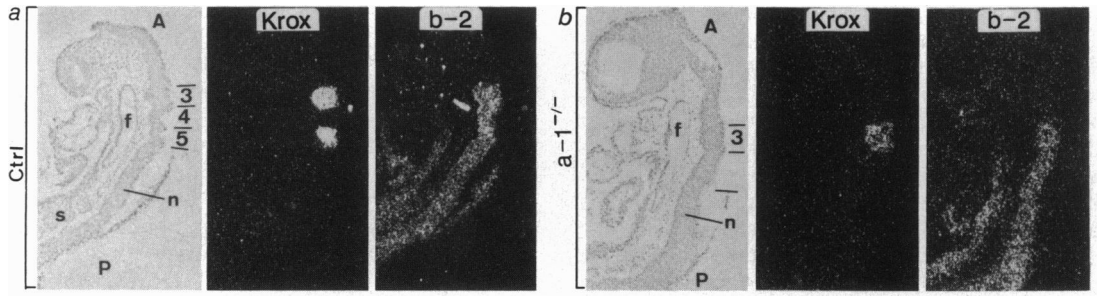

FIG. 1. *Krox-20* and *Hoxb-2* transcript domains in $Hoxa\text{-}1^{-/-}$ versus control embryos at E8.5. (*a*) Sagittal section of an E8.5 control ($Hoxa\text{-}1^{+/+}$) embryo hybridized to a *Krox-20* probe and photographed under bright-field light (for histology) and dark-field light (signal appears as white) as well as a consecutive section hybridized to a *Hoxb-2* probe (*Right*). (*b*) Consecutive sagittal sections of a $Hoxa\text{-}1^{-/-}$ littermate embryo hybridized to the same probes. The *Krox-20*-positive rhombomere, the match between *Hoxb-2* and *Krox-20* transcript boundaries, and the comparable *Hoxb-2* expression domains in both embryos define the existence of a r3 in $Hoxa\text{-}1^{-/-}$ embryos. Horizontal bars indicate rhombomere boundaries where visible on the sections shown, beginning with the r2/r3 boundary. Rhombomeres caudal to r3 are not numbered in the $Hoxa\text{-}1^{-/-}$ embryos, since they may not correspond to rhombomeres located at the same axial level in wild-type embryos (see text). A, anterior; P, posterior; 3–5, r3–r5; f, foregut; s, somites; n, neuroepithelium.

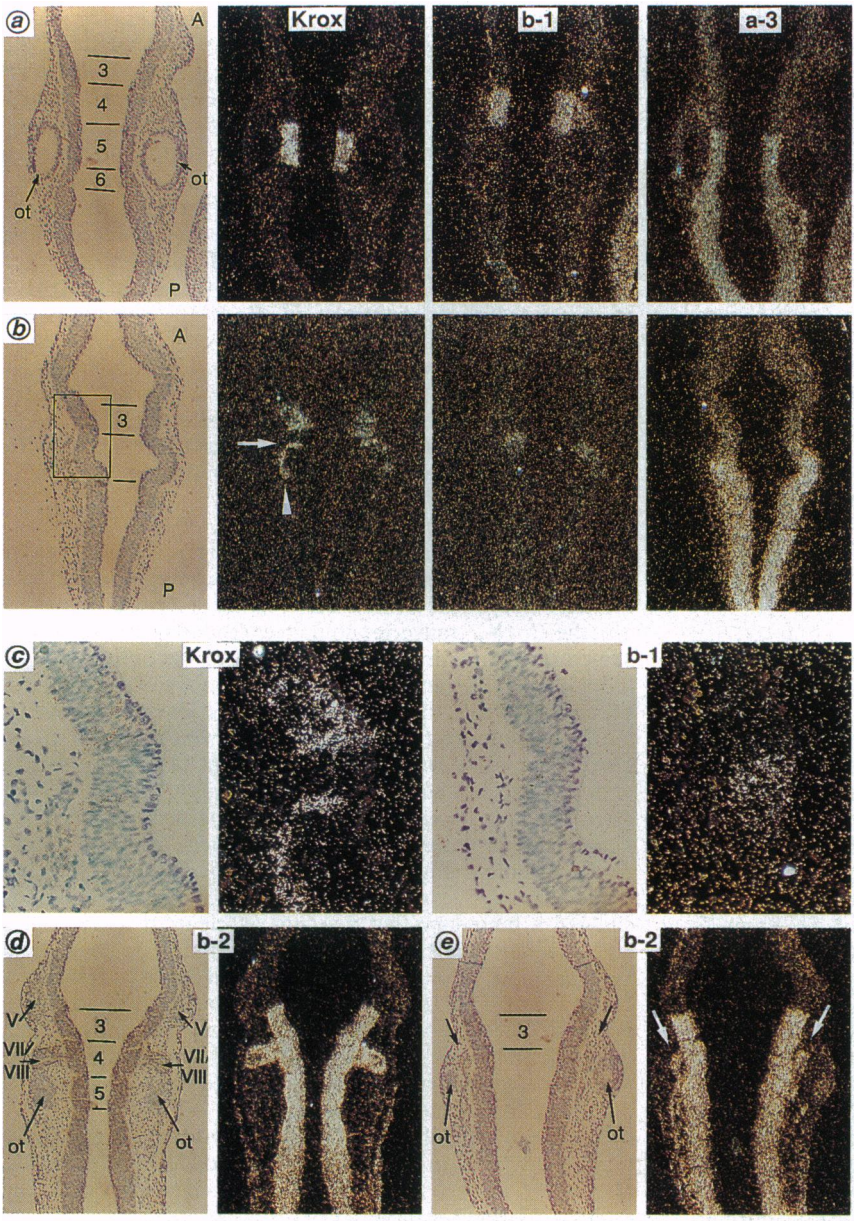

FIG. 2. *Krox-20*, *Hoxb-1*, and *Hoxa-3* expression and cranial ganglion morphology in *Hoxa-1*$^{-/-}$ embryos. (*a*) Coronal sections through an E9.5 control embryo hybridized to *Krox-20*, *Hoxb-1*, and *Hoxa-3* RNA probes. *Hoxb-1* and *Hoxa-3* have sharp expression limits on the two sides of the r4/r5 boundary. In this specimen, *Krox-20* expression has already disappeared from r3. In various E9.5 specimens, the *Krox-20* signal was either undetectable in r3 or weak and distorted (e.g., Fig. 2*b* or 3*a*). This is probably because the down-regulation of *Krox-20* in r3 is taking place at this time. (*b*) Coronal sections through an E9.5, *Hoxa-1*$^{-/-}$ embryo. The section is dorsal to the otocysts and shows the thin stripe of neuroepithelial cells expressing *Krox-20* posterior to r3—i.e., the vestige of r5 (arrow). Note also the thin population of *Krox-20*-labeled cells within the mesenchyme (arrowhead), which reveals that the small population of r5-derived neural crest (ref. 28; see Fig. 3*a*) is probably maintained in mutant embryos. In these embryos, *Hoxb-1* expression is weak and spatially reduced. It is nevertheless located just posterior to *Krox-20*-expressing cells in r3 and in between these and the *Krox-20* posterior stripe (*Left*). (*c*) High-power magnification of boxed area in *b*, showing spatial relationship between *Krox-20*- and *Hoxb-1*-expressing cells. (*d* and *e*) Coronal sections through the hindbrain of a control (*d*) and a *Hoxa-1*$^{-/-}$ (*e*) embryo hybridized to a *Hoxb-2* probe. Both sections cross the dorsal part of the otocysts. The *Hoxb-2* transcript anterior boundary in the mutant embryo is as in wild type, but the labeled facial–acoustic ganglion primordia have an altered morphology (arrows). A, anterior; P, posterior; 3–6, r3–r6; ot, otocyst; V, trigeminal ganglion; VII/VIII, facial–acoustic ganglion.

between mutant and control animals in terms of both tissue distribution and transcript abundance (e.g., Fig. 3 *c* and *d*; compare also the tail bud in Fig. 3 *a* and *b*). *Hoxb-2*, *Hoxb-3*, and *Hoxd-1* expression patterns, as well as the early and widespread expression of *Hoxb-1*, also remained unchanged (data not shown). Analysis of E10.5 and E12.5 embryos confirmed that these unaltered patterns of expression were maintained (data not shown).

The hindbrain neural crest and its derivatives, in particular the primordia of cranial nerve sensory ganglia, express various sets of *Hox* genes (26). As expected, in control embryos, the facial–acoustic ganglion complex, which is formed in part by r4-derived neural crest, was labeled by the *Hoxb-2* and *Hoxa-2* probes and was located anterior to the otocyst (Figs. 2*d* and 3*a*). In mutant embryos, however, this large ganglion complex was disorganized and its position was altered. Indeed, the *Hoxb-2*-labeled cells formed a narrow stripe adjacent and parallel to the neuroepithelium at the level of the otocyst (Figs. 2*e* and 3*b*, arrows; see also Fig. 4*b*). The presence of these neural crest cells between the neuroepithelium and the otocyst may be linked to the abnormal position of the otocyst, which normally faces a rhombomere with very few neural crest cells (r5; Figs. 2 *d* and *e* and 4*b*; see also refs. 23 and 28). Further detailed analysis of the alterations in neural crest and its derivatives will be reported elsewhere (31).

DISCUSSION

The present molecular analysis reveals that the *Hoxa-1* mutation generates a very precise disruption in the hindbrain rhombomeric pattern. Clearly, *Hoxa-1*$^{-/-}$ mice exhibit an abnormal distribution of *Krox/Hox* transcripts in a limited part of their hindbrain epithelium. r2 and r3 appear normal in mutant embryos, as judged by the *Hoxb-2*, *Hoxa-2*, and *Krox-20* transcript domains and boundaries. The alterations start precisely at the boundary between r3 and r4, which corresponds to the level of *Hoxa-1* anterior expression boundary in day-7.5 to -8.5 wild-type embryos (22) and are thus restricted to the most anterior subset of the *Hoxa-1* expression domain. Altogether, cells that have a genuine r4 combination of gene expression are severely reduced, and those exhibiting a genuine r5 combination are even more depleted since they consist of only a few cells located dorsally. In the mutant embryos, these r4–r5 cells are located at the level of the constriction that separates the third and

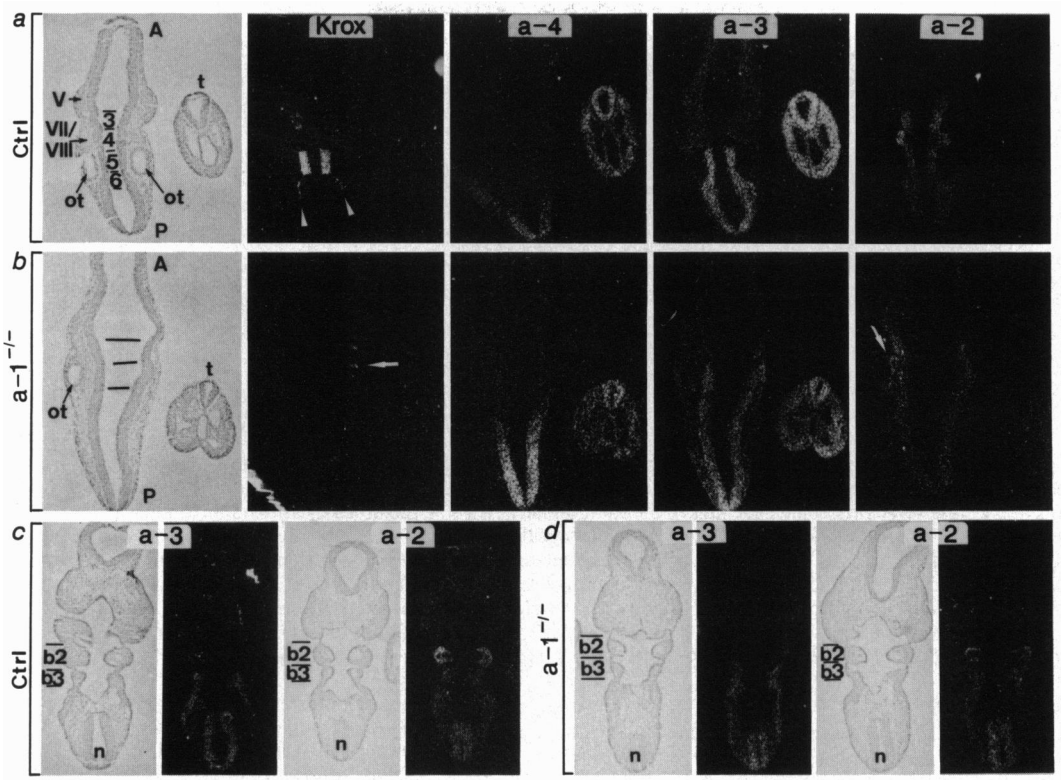

FIG. 3. *Hoxa* gene expression in *Hoxa-1*$^{-/-}$ versus control embryos at E9.5. (*a*) Coronal sections through the hindbrain of an E9.5 wild-type embryo crossing both otocysts and hybridized to *Krox-20*-, *Hoxa-4*-, *Hoxa-3*-, and *Hoxa-2*-specific RNA probes. All rhombomere bulges and boundaries are readily identified and can be numbered according to the otocyst position and molecular markers. At this stage, *Krox-20* expression is very weak in r3 but maximal in r5 and in a thin neural crest cell population originating from r5 (arrowheads; see ref. 28). *Hoxa-2* transcripts extend up to r2 and are more abundant in r3 and r5, *Hoxa-3* transcripts display a sharp cutoff at the r4/r5 boundary, and *Hoxa-4* transcripts show a more regular decrease toward the r6/r7 boundary. (*b*) Coronal sections through the hindbrain of an E9.5 mutant homozygote embryo. As these sections are dorsal and slightly tilted, only the left otocyst is visible, with the right side of the neuroepithelium being more dorsal. Note the very thin stripe of *Krox-20*-labeled cells in this dorsal area of the neuroepithelium (arrow). (*c*) Coronal sections through the branchial arches of two control E9.5 embryos, showing *Hoxa-3* (*Left*) and *Hoxa-2* (*Right*) transcript domains that extend anteriorly up to the third (*Hoxa-3*) and second (*Hoxa-2*) branchial arch. (*d*) Comparable coronal sections of two *Hoxa-1*$^{-/-}$ embryos. *Hoxa-3* and *Hoxa-2* transcript distribution is virtually identical to the controls and the respective transcript boundaries in the branchial arches are conserved. A, anterior; P, posterior; 3–6, r3–r6; ot, otocyst; t, tail bud; V, trigeminal ganglion; VII/VIII, facial–acoustic ganglion complex; b2 and b3, branchial arches 2 and 3; n, neural tube.

fourth rhombomere, as well as in the most anterior part of the fourth rhombomere (see Fig. 4*b*). Thus, the major part of the mutant fourth rhombomere, which is facing the otocyst, harbors a r6-like combination (i.e., the presence of *Hoxa-3* and *Hoxb-3* without *Krox-20*; see Fig. 4*b*). Therefore, the *Hoxa-1* loss of function has apparently resulted in a limited deletion of the hindbrain epithelium—namely, of the major part of normal r4 and r5. That r4 and r5 are markedly reduced in *Hoxa-1*$^{-/-}$ embryos is further supported by morphological and histological analyses of the hindbrain, neural crest cell migration, and nerve patterns in these embryos (31). For instance, mutant embryos lack the neural crest-free area at the expected position of r5, and the facial–acoustic neural crest cells appear continuous with putative glossopharyngeal–vagus neural crest cells (Figs. 2*e* and 4*b*; ref. 31).

The second conclusion to be drawn from this study is that the lack of a functional *HoxA-1* product does not significantly alter the correct activation and regulation of other *Hoxa* and *Hoxb* genes. The distribution of several *Hoxa* and *Hoxb* transcripts was studied (results summarized in Fig. 4), and no significant qualitative or quantitative alterations of their expression could be detected in any region of the *Hoxa-1*$^{-/-}$ embryos. Obviously, we cannot exclude the possibility that the *HoxA-1* protein could control the expression of *Hox* genes (e.g., *Hoxb-1*), which are normally expressed in the two rhombomeres (r4 and r5) that are markedly reduced in *Hoxa-1*$^{-/-}$ embryos. Although *Hoxa-1* is located at the 3′ extremity of the *HoxA* complex and is one of the earliest and anteriormost expressed *Hox* genes (1, 22), its expression is clearly not a prerequisite for correct expression of more 5′-located *Hoxa* genes or of their paralogous genes. Altogether, these results suggest that there are no significant regulatory effects of a *Hox* gene product on the expression of more-posterior (5′ located) genes. Alternatively, if such a regulation existed, one would have to assume that it can also be exerted by paralogous Hox proteins expressed simultaneously and in similar domains (for instance, *Hoxa-1* and *Hoxb-1*). In this case, a deregulation of *Hox* gene expression might be observed only in embryos mutated for both *Hoxa-1* and *Hoxb-1*.

The mechanism by which a lack of the *HoxA-1* homeoprotein can lead to a restricted deletion of the hindbrain epithelium remains to be elucidated. Basically, two types of hypotheses that are not mutually exclusive can be proposed. The first possibility would be that *HoxA-1* function is directly responsible for correct specification of a limited region of the hindbrain epithelium (corresponding to r4 and r5). In the absence of a *HoxA-1* product, the lack of specification of r4 and r5 (or the wrong specification) would ultimately lead to the apoptosis of most of the cells that normally constitute r4 and r5. Because there are some cells that express r4 and r5 markers (*Hoxb-1* and *Krox-20*), it appears that the mutation of *Hoxa-1* does not prevent all aspects of a *Hox* code for r4 and r5 from being initially activated. The second possibility

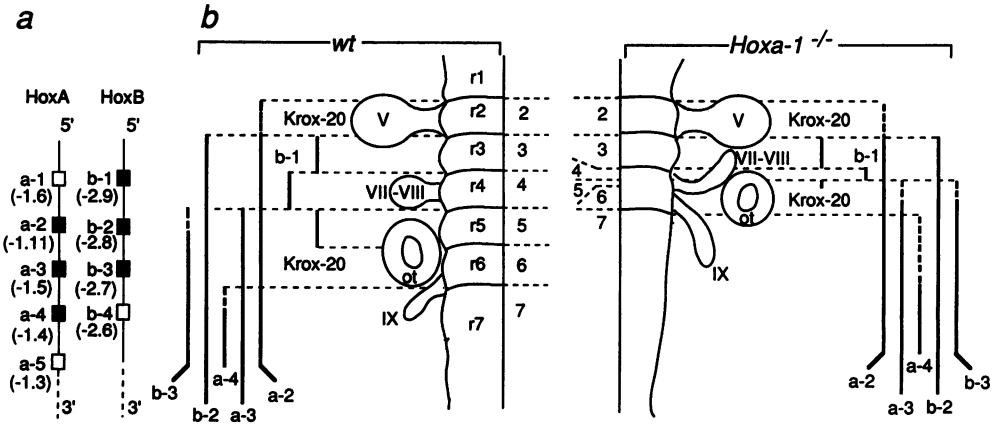

FIG. 4. (*a*) Scheme of the 3' regions of the *HoxA* and *HoxB* complexes indicating positions of various genes and their structural relationships (paralogous genes are aligned horizontally). Solid boxes correspond to the genes analyzed in this study. (*b*) Wild-type (*Left*) and *Hoxa-1*$^{-/-}$ (*Right*) hindbrains at E9.5 are schematized by drawings of the rhombomeres (r2–r7), the otocyst (ot), and three neural crest-derived cranial nerve ganglia (V, trigeminal; VII–VIII, facial–acoustic; IX, glossopharyngeal). In *Hoxa-1* mutants, five rhombomeres have been morphologically identified and the otocyst is facing the fourth one (ref. 31). The extents of the gene expression domains are represented by heavy vertical lines on either side. Dashed vertical lines indicate weak expression and/or an ill-defined boundary. In the central part, the potential rhombomeric identities as defined by the particular combination of *Hox/Krox* transcripts are shown for the control embryo (*Left*; 2–7). Rhombomeres of the mutant embryo are assigned with potential identities that reflect the particular combinations of the *Hox/Krox* genes they express. This illustrates the reduction in size of r4 and the almost complete absence of cells expressing a r5 combination.

is that the *HoxA-1* product may actively be involved in maintaining or regulating the correct growth of the hindbrain epithelium in this limited area. This is not incompatible with the possibility that the *HoxA-1* product may also act as a determinant of rhombomere-specific identity in a way similar to the *Drosophila* homeotic proteins. Such a possibility may be exemplified by the phenotypic alterations observed in r6-derived structures, which may result from an incorrect determination of the cells of this rhombomere due to the absence of the *HoxA-1* product. We feel that the early molecular changes in hindbrain segmentation presented in this study provide insight into the primary nature of the mutant phenotype. Proper patterning of rhombomeres is clearly important for generation of normal morphological structures in the branchial region of the head.

We are grateful to Dr. P. Charnay for the gift of the *Krox-20* probe. We thank V. Friederich-Fraulob and N. Chartoire for efficient technical assistance; B. Boulay, C. Werlé, and the European Molecular Biology Laboratory photolab for illustration work; and the secretarial staff for preparing the manuscript. This work was supported by funds from the Human Science Frontier Program Organisation, the Institut National de la Santé et de la Recherche Médicale, the Centre National de la Recherche Scientifique, the Centre Hospitalier Universitaire Régional, the Association pour la Recherche sur le Cancer, and the Fondation pour la Recherche Médicale.

1. Duboule, D. & Dollé, P. (1989) *EMBO J.* **8**, 1497–1505.
2. Graham, A., Papalopulu, N. & Krumlauf, R. (1989) *Cell* **57**, 367–378.
3. Scott, M. P. (1992) *Cell* **71**, 551–553.
4. Kessel, M. & Gruss, P. (1991) *Science* **249**, 374–379.
5. McGinnis, W. & Krumlauf, R. (1992) *Cell* **68**, 282–302.
6. Gaunt, S. J., Sharpe, P. T. & Duboule, D. (1988) *Development* **104**, Suppl., 71–82.
7. Dollé, P., Izpisùa-Belmonte, J.-C., Falkenstein, H., Renucci, A. & Duboule, D. (1989) *Nature (London)* **342**, 767–772.
8. Yokouchi, Y., Sasaki, H. & Kuroiwa, A. (1991) *Nature (London)* **353**, 443–445.
9. Dollé, P., Izpisùa-Belmonte, J.-C., Brown, J. M., Tickle, C. & Duboule, D. (1991) *Genes Dev.* **5**, 1767–1776.
10. Balling, R., Mutter, G., Gruss, P. & Kessel, M. (1989) *Cell* **58**, 337–347.
11. Morgan, B. A., Izpisùa-Belmonte, J.-C., Duboule, D. & Tabin, C. (1992) *Nature (London)* **358**, 236–239.
12. Lufkin, T., Mark, M., Hart, C. P., Dollé, P., LeMeur, M. & Chambon, P. (1992) *Nature (London)* **359**, 835–841.
13. Chisaka, O. & Capecchi, M. R. (1991) *Nature (London)* **350**, 473–479.
14. Lufkin, T., Dierich, A., LeMeur, M., Mark, M. & Chambon, P. (1991) *Cell* **66**, 1105–1120.
15. Chisaka, O., Musci, T. S. & Capecchi, M. R. (1992) *Nature (London)* **355**, 516–521.
16. LeMouellic, H., Lallemand, Y. & Brûlet, P. (1992) *Cell* **69**, 251–264.
17. Han, K., Levine, M. S. & Manley, J. L. (1989) *Cell* **56**, 573–583.
18. Krasnow, M. A., Saffman, E. E., Kornfeld, K. & Hogness, D. S. (1989) *Cell* **57**, 1031–1043.
19. Winslow, G. M., Hayashi, S., Krasnow, M., Hogness, D. S. & Scott, M. P. (1989) *Cell* **57**, 1017–1030.
20. Zappavigna, V., Renucci, A., Izpisùa-Belmonte, J.-C., Urier, G., Peschle, C. & Duboule, D. (1991) *EMBO J.* **10**, 4177–4187.
21. Arcioni, L., Simeone, A., Guazzi, S., Zappavigna, V., Boncinelli, E. & Mavilio, F. (1992) *EMBO J.* **11**, 265–278.
22. Murphy, P. & Hill, R. E. (1991) *Development* **111**, 61–74.
23. Lumsden, A. (1990) *Trends Neurosci.* **13**, 329–336.
24. Gaunt, S. J., Miller, J. R., Powell, D. J. & Duboule, D. (1986) *Nature (London)* **324**, 662–664.
25. Wilkinson, D. G., Bhatt, S., Cook, M., Boncinelli, E. & Krumlauf, R. (1989) *Nature (London)* **341**, 405–409.
26. Hunt, P., Gulisano, M., Cook, M., Sham, M., Faiella, A., Wilkinson, D. G., Boncinelli, E. & Krumlauf, R. (1991) *Nature (London)*.**353**, 861–864.
27. Dollé, P. & Duboule, D. (1989) *EMBO J.* **8**, 1507–1515.
28. Sham, M. H., Vesque, C., Nonchev, S., Marshall, H., Frain, M., Das Gupta, R., Whiting, J., Wilkinson, D., Charnay, P. & Krumlauf, R. (1993) *Cell* **72**, 183–196.
29. Murphy, P., Davidson, D. & Hill, R. E. (1989) *Nature (London)* **341**, 156–159.
30. Frohman, M. A., Boyle, M. & Martin, G. R. (1990) *Development* **110**, 589–607.
31. Mark, M., Lufkin, T., Vonesch, J. L., Ruberte, E., Olivo, J. C., Dollé, P., Gorry, P., Lumsden, A. & Chambon, P. (1993) *Development*, in press.